Neuroimaging of hypothalamic mechanisms related to glucose metabolism in anorexia nervosa and obesity

Joe J. Simon,[1,2] Marion A. Stopyra,[1] Esther Mönning,[1] Sebastian Sailer,[1] Nora Lavandier,[1] Lars P. Kihm,[3] Martin Bendszus,[4] Hubert Preissl,[5,6,7,8,9,10] Wolfgang Herzog,[1] and Hans-Christoph Friederich[1,2]

[1]Centre for Psychosocial Medicine, Department of General Internal Medicine and Psychosomatics, University Hospital Heidelberg, Heidelberg, Germany. [2]Department of Psychosomatic Medicine and Psychotherapy, Medical Faculty, Heinrich Heine University Düsseldorf, Düsseldorf, Germany. [3]Endocrinology and Nephrology, Department of Internal Medicine I, and [4]Department of Neuroradiology, University Hospital of Heidelberg, Heidelberg, Germany. [5]fMEG Center, Helmholtz Center Munich, University of Tübingen, Tübingen, Germany. [6]Institute for Diabetes Research and Metabolic Diseases of the Helmholtz Center Munich (IDM) at the University of Tübingen, Tübingen, Germany. [7]German Center for Diabetes Research (DZD e.V.), Tübingen, Germany. [8]Division of Endocrinology, Diabetology, Angiology, Nephrology and Clinical Chemistry, Department of Internal Medicine, University Hospital Tübingen, Tübingen, Germany. [9]Department of Pharmacy and Biochemistry, Interfaculty Centre for Pharmacogenomics and Pharma Research, University of Tübingen, Tübingen, Germany. [10]Institute for Diabetes and Obesity, Helmholtz Diabetes Centre, Helmholtz Centre Munich, German Research Centre for Environmental Health (GmbH), Neuherberg, Germany.

BACKGROUND. Given the heightened tolerance to self-starvation in anorexia nervosa (AN), a hypothalamic dysregulation of energy and glucose homeostasis has been hypothesized. Therefore, we investigated whether hypothalamic reactivity to glucose metabolism is impaired in AN.

METHODS. Twenty-four participants with AN, 28 normal-weight participants, and 24 healthy participants with obesity underwent 2 MRI sessions in a single-blind, randomized, case-controlled crossover study. We used an intragastric infusion of glucose and water to bypass the cephalic phase of food intake. The responsivity of the hypothalamus and the crosstalk of the hypothalamus with reward-related brain regions were investigated using high-resolution MRI.

RESULTS. Normal-weight control participants displayed the expected glucose-induced deactivation of hypothalamic activation, whereas patients with AN and participants with obesity showed blunted hypothalamic reactivity. Furthermore, patients with AN displayed blunted reactivity in the nucleus accumbens and amygdala. Compared with the normal-weight participants and control participants with obesity, the patients with AN failed to show functional connectivity between the hypothalamus and the reward-related brain regions during water infusion relative to glucose infusion. Finally, the patients with AN displayed typical baseline levels of peripheral appetite hormones during a negative energy balance.

CONCLUSION. These results indicate that blunted hypothalamic glucose reactivity might be related to the pathophysiology of AN. This study provides insights for future research, as it is an extended perspective of the traditional primary nonhomeostatic understanding of the disease.

FUNDING. This study was supported by a grant from the DFG (SI 2087/2-1).

Introduction

A fundamental question in anorexia nervosa (AN) research is to understand how patients resist food intake despite being life-threateningly underweight (1). Previous neuroscientific research has primarily focused on food cue presentation and taste perception paradigms, assessing mainly nonhomeostatic factors related to the pathophysiology of AN. It has been argued that an overactive cognitive control network combined with alterations in reward, emotional, and interoceptive information processing contribute to decreased food intake and heightened tolerance to physical hunger in AN (2). However, the impact of homeostatic mechanisms, including their crosstalk with nonhomeostatic factors in the development and maintenance of AN, remains largely unknown (3). In contrast to individuals with constitutional thinness, patients with AN show typical physiological adaptations to a negative energy balance in peripheral hunger and satiety hormones (4). Nonetheless, these metabolic signals do not result in adaptive strategies for regaining a neutral or positive energy balance (5). Therefore, these adaptations are thought to contribute to the maintenance of AN, given their influence over neuronal networks related to food processing (6). Similarly, abnormalities in hormonal satiety signaling are considered a hallmark feature in the etiology of obesity, in which the hypothalamus becomes less sensitive to peripheral anorexigenic as well as orexigenic signaling, leading to increased food intake (7). Furthermore, previous imaging studies have demonstrated that hyperresponsivity of the reward system to food stimuli is a risk factor for nonhomeostatic eating, which has been associated with the development and maintenance of obesity (8). However, gut/brain signaling and

Conflict of interest: The authors have declared that no conflict of interest exists.

Submitted: January 28, 2020; **Accepted:** April 16, 2020; **Published:** June 22, 2020.
Reference information: *J Clin Invest*. 2020;130(8)4094–4103.
https://doi.org/10.1172/JCI136782.

Table 1. Demographic and clinical characteristics of participants

Variable	Normal-weight controls (*n* = 28)	Patients with AN (*n* = 24)	Controls with obesity (*n* = 24)	AN vs. CON *P* value[A]	OB vs. CON *P* value[B]	OB vs. AN *P* value[C]
Age, mean (SD), yr	24.6 (4.95)	23.48 (4.95)	27.13 (5.97)	0.414	0.103	0.007
BMI (SD)	21.87 (1.27)	15.48 (1.5)	35.66 (3.83)	< 0.001	< 0.001	< 0.001
Education, mean (SD), yr	12.78 (0.78)	12.37 (1.24)	12.12 (1.39)	0.155	0.078	0.478
BDI, mean (SD)	4.25 (3.66)	21 (14.24)	11.37 (8.16)	< 0.001	< 0.001	0.009
EDEQ total score, mean (SD)	10 (9.02)	81.92 (34.46)	56.58 (21.96)	< 0.001	< 0.001	0.003
EDEQ restraint, mean (SD)	2 (3.75)	18.42 (8.38)	9.95 (6.27)	< 0.001	<0.001	<0.001
EDEQ eating concern, mean (SD)	0.43 (0.69)	14.83 (7.9)	6 (4.66)	< 0.001	<0.001	<0.001
EDEQ weight concern, mean (SD)	2.46 (2.09)	17.25 (8.55)	14.33 (5.69)	<0.001	<0.001	0.142
EDEQ shape concern, mean (SD)	5.12 (5.11)	31.42 (12.97)	26.29 (10.62)	<0.001	<0.001	0.167

All participants were women. [A]The *P* values presented relate to unpaired, 2-sample Student's *t* test comparing normal-weight controls and patients with AN. [B]The *P* values presented relate to unpaired, 2-sample Student's *t* tests comparing participants with obesity and normal-weight controls. [C]The *P* values presented relate to unpaired, 2-sample Student's *t* tests comparing participants with obesity and patients with AN. BDI, Beck Depression Inventory; EDEQ, Eating Disorder Examination Questionnaire; CON, normal-weight controls; AN, patients with anorexia nervosa; OB, controls with obesity.

homeostatic glucose processing in adult obesity is largely unexplored, with only a few studies investigating the hypothalamic response to oral glucose infusion (9, 10).

The hypothalamus and brainstem regions are crucial in monitoring energy balance through a number of hormonal and neural nutrient-sensing mechanisms that allow accurate and stable energy and body weight regulation (11). Gastric peptides interact with the mesocorticolimbic reward circuitry via the hypothalamus to modulate the rewarding aspects of food intake (12). Specifically, the nucleus accumbens (NAcc) is instrumental in encoding the reinforcing value of food, a process that has been found to be partially regulated via glucose metabolism (13, 14). Similarly, the amygdala has previously been associated with anticipatory food reward processing (15), and activity levels in this region have been found to be influenced by hormonal satiety signaling (16). The lateral hypothalamus and brainstem regions have subgroups of neurons that are specifically responsible for sensing and regulating glucose levels (17). Previous studies found that the hypothalamus responds with decreased activity upon administration of glucose (18, 19). However, the investigation of in vivo hypothalamic responses to nutrient infusion using functional MRI (fMRI) is challenging. At present, the extent to which the hypothalamus as the core region for homeostatic regulation is involved in the pathophysiology of individuals with AN remains largely unknown (20).

In the present study, we used high-resolution fMRI with an optimized protocol for the hypothalamus and mesocorticolimbic reward system to study the small-sized hypothalamus localized around the third ventricle. Furthermore, we used a single-blind, randomized crossover design of an intragastric infusion of glucose and water to bypass the cephalic phase of food intake (i.e., sight, smell, taste). Inclusion of normal-weight and obese control groups allowed us to differentiate hypothalamic reactivity to glucose across a wide range of BMIs. Taken together, the aim of this study was to gain insights into glucose-induced hypothalamic reactivity as well as the crosstalk between the hypothalamus and the mesocorticolimbic reward network in patients with AN.

Results

Behavioral and subject data. Demographic and clinical characteristics of the study participants are provided in Table 1. Two normal-weight participants and 1 control participant with obesity had to be excluded because of technical difficulties or excessive head movement during scanning (Figure 1). The participants remained unaware of the type of liquid administered during each session, since all 3 groups guessed at chance level at the first (healthy controls, $\chi^2 = 0.465$, $P = 0.495$; AN, $\chi^2 = 0.621$, $P = 0.431$; controls with obesity, $\chi^2 = 0.168$, $P = 0.682$) and second (healthy controls, $\chi^2 = 2.707$, $P = 0.1$; AN, $\chi^2 = 1.731$, $P = 0.188$; controls with obesity, $\chi^2 = 0.011$, $P = 0.916$) visits. All participants rated their subjective sensation of hunger before and after each session. A repeated-measures ANOVA with liquid type (infusion of water or glucose) and time point (before or after infusion of water or glucose) as within-subject factors and group as a between-subjects factor revealed an effect of liquid type on hunger ratings ($P = 0.026$) but no effect of time point ($P = 0.287$). There was no interaction between group and liquid type ($P = 0.293$), but there was a significant interaction between group and time point ($P = 0.047$). Post hoc tests revealed that both normal-weight controls as well as patients with AN failed to show differences in hunger ratings before and after each session (normal-weight controls, all *P* values [*P*s] > 0.059; patients with AN, all *P*s > 0.117). However, controls with obesity showed an increase in hunger ratings after the infusion of water ($P = 0.007$). When comparing pre- and postinfusion differences in hunger ratings between groups, we observed no differences between normal-weight controls and patients with AN (*P*s > 0.06) or between controls with obesity and patients with AN (*P*s > 0.352).

Hormonal satiety parameters. Because of technical difficulties, blood samples were not collected for all participants, and the respective group sizes are indicated in Table 2. As expected, patients with AN showed typical hormonal adaptions to a negative energy balance with decreased blood plasma leptin and insulin and increased serum-active ghrelin levels. Taken together, although we observed some differences between groups in baseline or postinfusion levels, the infusion of glucose increased blood glucose and insulin levels and decreased active ghrelin

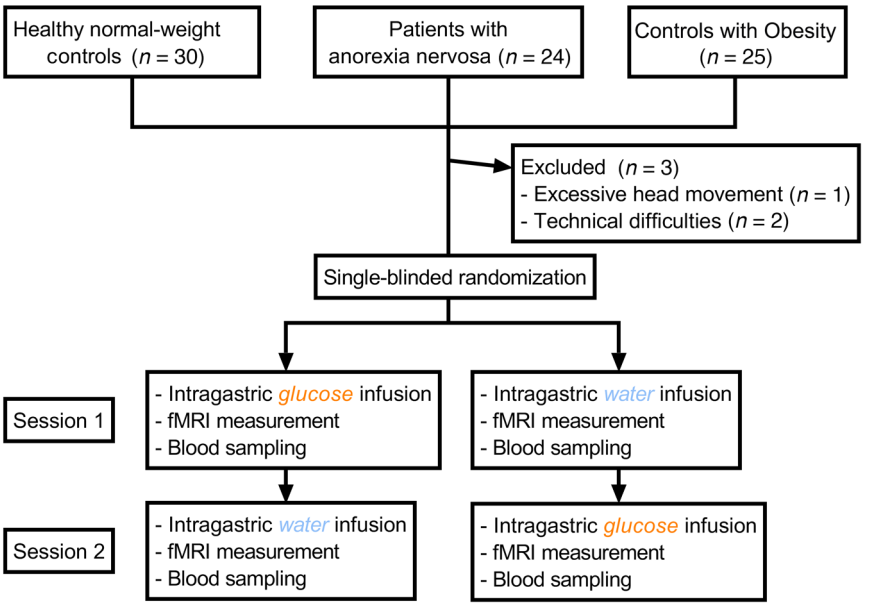

Figure 1. Study design. We used a randomized, single-blind, crossover experimental fMRI design of intragastric glucose versus water infusion via a nasogastric tube. Normal-weight control participants were matched to patients with AN and control participants with obesity with regard to age and education level. Blood samples used to determine hormonal satiety parameters were obtained 30 minutes before and 45 minutes after liquid infusion.

levels in comparable proportions in all 3 groups (detailed results are provided in Table 2).

Structural brain differences. Hypothalamic volumetric differences between groups are detailed in the Supplemental Results (Supplemental material available online with this article; https://doi.org/10.1172/JCI136782DS1). In short, we observed no difference in hypothalamic volume (calculated as a percentage of total brain volume) between normal-weight controls and patients with AN, but we observed an increased hypothalamic volume in normal-weight controls when compared with controls with obesity. However, we found no difference in hypothalamic volume between patients with AN and controls with obesity.

Glucose and water induced BOLD activation in homeostatic and reward-related brain regions. Normal-weight control participants showed the expected glucose-induced attenuation of hypothalamic activity: a comparison of the AUC revealed significant differences in hypothalamic activity between glucose and water infusion (t_{27} = 3.58, P = 0.001). However, glucose infusion in patients with AN and controls with obesity failed to reduce hypothalamic activity (AN, t_{23} = 1.98, P = 0.059; controls with obesity, t_{23} = 0.741, P = 0.465; Figure 2). Furthermore, activation in the NAcc and amygdala was attenuated by glucose infusion in the normal-weight controls, but not in the patients with AN or the controls with obesity (see Figures 3 and 4 for detailed results). A group comparison of hypothalamus activation revealed significant differences between all 3 groups in the blood oxygen level–dependent (BOLD) signal response in the hypothalamus during glucose infusion ($F_{2,73}$ = 5.74, P = 0.005; Figure 5), with a stronger deactivation in normal-weight controls when compared with patients with AN (t_{50} = 2.52, P = 0.015) and when compared with controls with obesity (t_{50} = 2.75, P = 0.008), but no significant difference between controls with obesity and patients with AN (P = 0.911). No significant correlation was observed between signal response in the hypothalamus and hormonal satiety parameters in the 3 groups combined (Ps > 0.169), or in the group of normal-weight controls (Ps > 0.06), the group of patients with AN (Ps > 0.129), or the group of controls with obesity (Ps > 0.418).

Group comparisons of NAcc and amygdala activations revealed significant differences between groups in BOLD signal response in the NAcc and the amygdala during glucose infusion (Figure 5). Furthermore, we analyzed activation in the caudate nucleus (the dorsal part of the striatum), putamen (encompassing most of the ventral part of the striatum), insular cortex, medial orbitofrontal cortex, and inferior operculum (corresponding to the primary gustatory cortex). We found significant deactivation in all regions of interest in normal-weight controls, but no significant deactivation in any of the regions in the control participants with obesity or the patients with AN. We observed significant group differences for the caudate nucleus, putamen, and insular cortex, but no group differences for the medial orbitofrontal cortex and inferior operculum. Post hoc tests revealed no significant differences between normal-weight control participants and patients with AN with regard to BOLD signal response in the caudate nucleus, putamen, and insular cortex. Detailed results are provided in the Supplemental Results.

Satiety state–dependent functional connectivity from the hypothalamus to reward-related brain regions. Normal-weight controls and participants with obesity displayed increased functional connectivity from the hypothalamus to reward-related brain regions after water infusion when compared with glucose infusion (ventral striatum, medial orbitofrontal cortex, insula, P < 0.05 significance threshold, FWE whole-brain corrected; Supplemental Figure 3). Participants with obesity showed increased functional connectivity in the primary gustatory cortex after the infusion of glucose. In patients with AN, we observed a reduced connectivity profile, with only the posterior insula showing increased connectivity with the hypothalamus after water infusion (Supplemental Figure 3). Analysis of group differences revealed differences between normal-weight controls and patients with AN in functional connectivity between the hypothalamus and left

Table 2. Differences in hormonal satiety parameters before and after the infusion of glucose

Variable	Normal-weight controls		Patients with AN		Controls with obesity		CON vs. AN vs. OB *P* value[A]	AN vs. CON *P* value[A]	OB vs. AN *P* value[A]
	Baseline	Glucose	Baseline	Glucose	Baseline	Glucose			
Blood glucose, mg/dL	84.7 ± 5.7	146.2 ± 17.9[D]	82.4 ± 7.9	140.1 ± 26.3[D]	85 ± 5.9	136.5 ± 23.8[D]	0.176	0.966	0.146
Insulin, mU/L[B]	7.8 ± 3.2	57.5 ± 28.9[D]	4.3 ± 3.2	37.9 ± 18.6[D]	14.8 ± 7.3	102.1 ± 64.5[D]	0.021	0.026	0.012
HOMA-IR	1.9 ±.92		1.02 ± 75		3.1 ± 1.5		< 0.001	0.001	< 0.001
Leptin, μg/L	8.5 ± 5.8	1.6 ± 1.2	1.6 ± 1.2		36.9 ± 16.1		< 0.001	< 0.001	< 0.001
Active ghrelin, pg/mL[C]	631.2 ± 371.4	310.5 ± 209.2[D]	1027.3 ± 543.3	407.8 ± 235.9[D]	410.6 ± 305.4	182 ± 144.4[D]	< 0.001	0.017	0.002

[A]*P* values relate to repeated-measures ANOVAs with time point (before and after glucose infusion) as a within factor and group as a between factor. [B]Additional post hoc tests revealed that patients with AN had different insulin baseline values compared with those for normal-weight healthy controls and controls with obesity (*P*s < 0.002), as well as different values after infusion (*P*s < 0.015). Baseline-corrected differences in insulin levels before and after infusion (postinfusion levels divided by preinfusion levels) revealed no significant differences between patients with AN and healthy controls (t_{44} = –1.38, *P* = 0.173) but significant differences between patients with AN and controls with obesity (t_{39} = 2.25, *P* = 0.03). [C]Additional post hoc tests revealed that patients with AN had different baseline values compared with those for healthy controls and controls with obesity (*P*s < 0.007), but the values after infusion were different only when compared with those for controls with obesity (t_{39} = 2.76, *P* = 0.009) and not when compared with those for normal-weight healthy controls (t_{44} = 0.37, *P* = 0.709). Baseline-corrected differences in active ghrelin levels before and after infusion (postinfusion levels divided by preinfusion levels) revealed no significant differences between patients with AN and normal-weight healthy controls (t_{40} = 1.58, *P* = 0.122) or between patients with AN and controls with obesity (t_{37} = –1.78, *P* = 0.084). [D]*P* ≤ 0.001, by paired, 2-tailed Student's *t* test.

ventral striatum and differences between normal-weight controls and controls with obesity in functional connectivity between the hypothalamus and brainstem. We also observed differences between patients with AN and controls with obesity in functional connectivity between the hypothalamus and left ventral striatum (see Figure 6). Supplemental Tables 1 and 2 indicate additional clusters of activation that emerged from the within-group and between-groups analyses.

Discussion

This study investigated glucose-induced hypothalamic reactivity in patients with AN in comparison with reactivity in both normal-weight controls and controls with obesity. Using a single-blind nasogastric infusion of glucose and water, we found that, compared with normal-weight controls, the patients with AN and controls with obesity showed diminished responses in the hypothalamus, ventral striatum, and amygdala following glucose infusion. Furthermore, normal-weight healthy participants and participants with obesity showed satiety state–dependent connectivity between the hypothalamus and mesocorticolimbic reward circuitry, whereas patients with AN did not. To our knowledge, this is the first brain imaging study that directly compares the glucose-induced hypothalamic reactivity of participants with normal weight, obesity, and AN.

In recent decades, neurobiological research delivered new insights into the mechanisms of metabolic and hormonal gut/brain signaling (21, 22). In particular, experimental research in animals has led to a profound understanding of the major factors that determine homeostatic and energy balance regulation (23). Under a negative energy balance, a number of adaptive strategies for regaining a neutral or positive energy balance are triggered via the gut/brain axis. There is a plethora of evidence linking hypothalamic dysregulation to the development and progression of obesity (24), whereby neural inflammation in the hypothalamus causes alterations in hypothalamic circuitry and outputs to other brain areas (25). On the other hand, an involvement of hypothalamic dysregulation in the pathophysiology of self-starvation in AN has just recently emerged as a growing area of research interest (26, 27). Our observation of blunted hypothalamic reactivity to intragastric infusion of glucose supports a pivotal role of hypothalamic dysfunction in AN and is in line with previous reports of a central nervous resistance to hormonal satiety in AN (28). Importantly, since both the patients with AN and controls with obesity displayed similar glucose-induced changes in hormonal signaling when compared with the normal-weight control group (i.e., an increase in insulin and blood glucose, but a decrease in ghrelin values), the observed blunted hypothalamic reactivity was less likely to be triggered by differences in the peripheral metabolism of glucose. Therefore, our results point toward a diminished central neuronal reaction to glucose metabolism in obesity and AN.

However, patients with AN differed from controls with obesity in the crosstalk between the hypothalamus and the reward system. During glucose infusion, the controls with obesity showed increased connectivity, whereas the patients with AN showed decreased connectivity with brain regions involved in reward processing. In patients with AN, an impaired crosstalk between the hypothalamus and the mesocorticolimbic reward system may lead to a partial or even complete loss of the hypothalamic regulation of food intake. Homeostatic hunger is known to increase brain activation in the reward system in response to exteroceptive food cues (29, 30), which further corroborates the close interaction between the hypothalamus and the neural reward network (14). Therefore, our results indicate that gut/brain signaling in AN is characterized by a blunted hypothalamic reactivity and concurrent reduced coding of hedonic and motivational aspects of food. Furthermore, our findings suggest that patients with AN have difficulties in differentiating between physical hunger and satiety and depend to a greater extent on the cephalic phase (i.e., sight, smell, taste) to

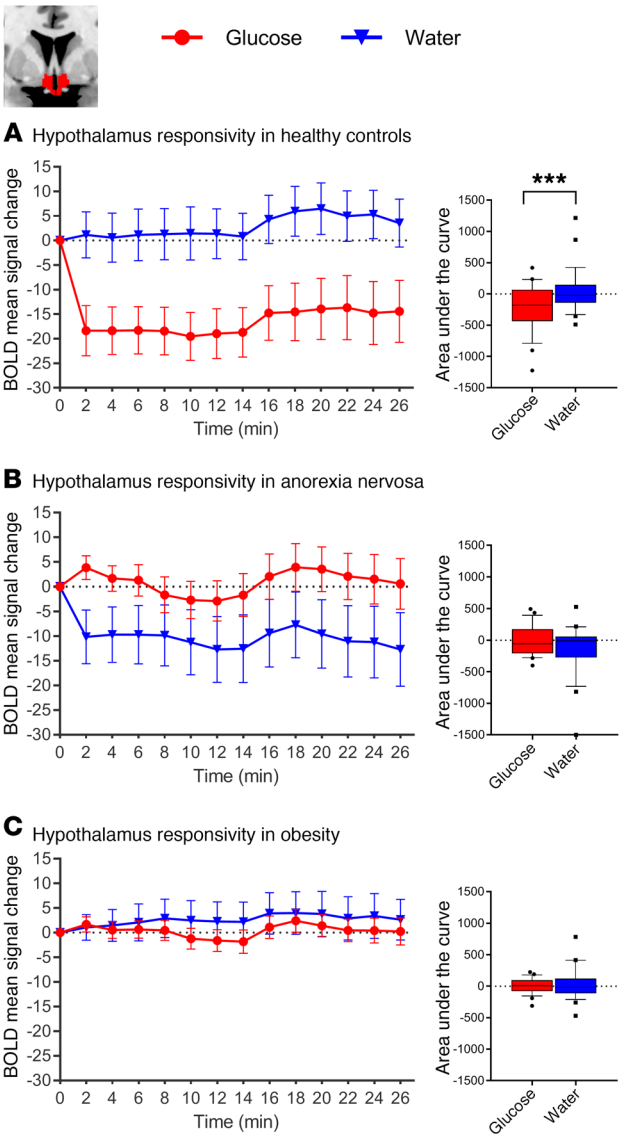

Figure 2. Changes in BOLD signal over time in response to glucose and water infusion in the hypothalamus. BOLD signal response in the hypothalamus ROI (manually segmented on individual native space brain scans) during glucose and water infusion. A comparison of the AUC revealed significant differences between treatment conditions in normal-weight healthy controls (**A**), but not in patients with AN (**B**) or controls with obesity (**C**). In the box-and-whisker plots, the horizontal bar indicates the median, the box edges represent the 25th and 75th percentiles, and the whiskers represent the 10th and 90th percentiles. ***$P \leq 0.001$, by paired, 2-tailed Student's *t* test.

regulate their food intake. This lack of homeostatic regulation may allow patients with AN to tolerate physical hunger despite being life-threateningly underweight. Our results are in support of and extend the long-held assumption of reduced food reward processing as a core neural mechanism underlying the development of AN (31). The blunted hypothalamic reactivity and reduced connectivity with brain reward regions point toward an inhibition of intuitive motivational responses to food stimuli (2, 32).

However, reduced hypothalamic reactivity to glucose infusion in obesity seems to be associated with an increased hedonic reactivity independent and decoupled from homeostatic signaling. This is in line with previous reports, in which an exaggerated neural reactivity of the reward network in response to high-calorie visual food cues and stronger functional connections between reward areas and the medial hypothalamus were observed in subjects with obesity (33, 34). Taken together, our results corroborate the assumption that a hyperresponsive reward system predominates the homeostatic regulation of food intake in obesity (35), potentially promoting overconsumption of high-calorie food via an increased motivational importance of food stimuli (36).

Limitations. Our study has several limitations. Since participants were given an infusion of glucose, we were unable to assess the effects of macronutrients on gut/brain signaling. Furthermore, future studies should assess trait and state aspects of impaired homeostatic signaling by including participants at risk of or recovered from AN or obesity. Since we included only women in our study, the observed results should be generalized to men with caution. Additionally, we did not control for the menstrual cycle in this study, which is a potential confounding factor, as it has previously been shown that neural food processing in women is influenced by the menstrual cycle (37). Moreover, since the hypothalamus is involved in the regulation of thirst (38) and has been associated with the development of dehydration-induced anorexia (39), the influence of dehydration on hypothalamic reactivity in AN should be explored in further studies. Although we used an fMRI acquisition procedure tailored to the small hypothalamic volume, its proximity to the sphenoid sinus makes the resulting images susceptible to inhomogeneities in the local magnetic field. Together with the fact that the hypothalamus is composed of nuclei with partially different functional properties, the fMRI method may not be able to completely assess this region. Additionally, the interaction between peripheral signals of energy homeostasis and neural reactivity is complex and remains incompletely understood (40). Despite the well-established response of the hypothalamus to glucose administration, there is uncertainty regarding the exact mechanisms underlying this reaction (41). Taken together, further research is necessary to replicate these preliminary findings and to study in more detail the influence of satiety states on the hypothalamus and on the interaction of the hypothalamus with the mesocorticolimbic reward system in AN.

Conclusions. The etiology and pathogenesis of AN are still largely unknown. By circumventing the cephalic phase of food consumption, the present study may support new paths in research by offering a role of altered reactivity in the pathophysiology of AN. By investigating the neural correlates of homeostatic regulation across the BMI spectrum in different satiety states, this study provides a better understanding of gut/brain signaling in human eating behavior. The findings suggest that, in addition to excessive self-regulatory control of food intake, blunted reactivity in the hypothalamus, NAcc, and amygdala may perpetuate self-starvation behaviors in AN. This is in line with current GWAS indicating fundamental metabolic dysregulation as a trait marker in AN (42). In addition to studies focusing primarily on nonhomeostatic neural mechanisms of food intake, further research is needed to understand alterations in the homeostatic regulation of food intake in AN.

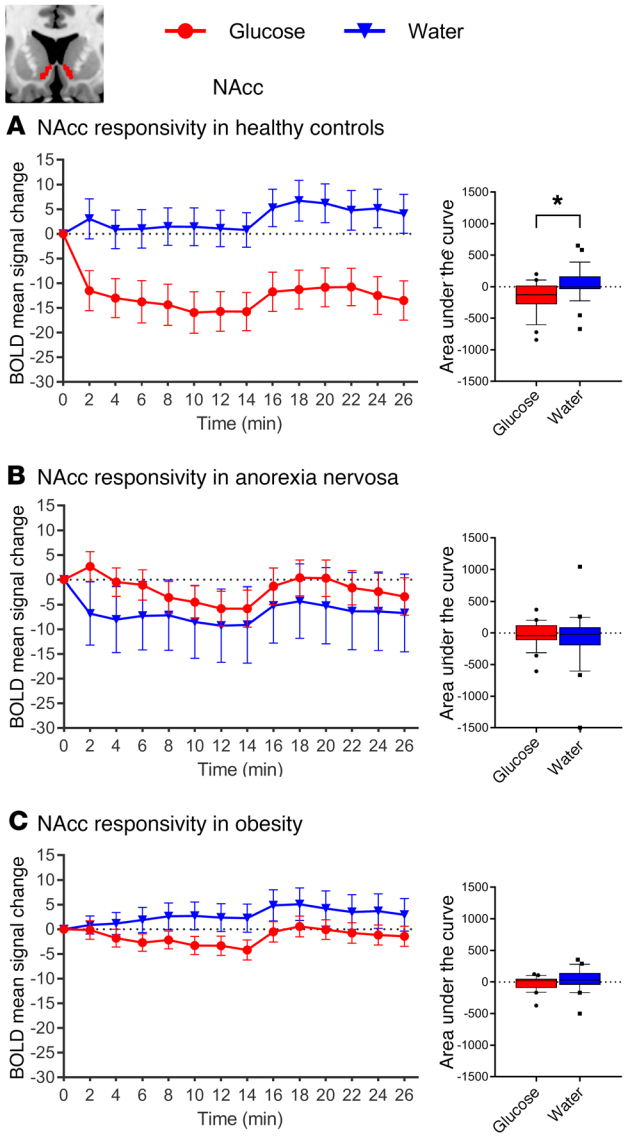

Figure 3. Changes in BOLD signal over time in response to glucose and water infusion in the NAcc. BOLD signal response in the NAcc ROI (automatic segmentation using FreeSurfer) during glucose and water infusion. Significant differences were observed between conditions in (**A**) normal-weight healthy controls (t_{27} = 3.31, P = 0.027), but not in (**B**) patients with AN (t_{23} = 0.665, P = 0.512) or (**C**) controls with obesity (t_{23} = 1.94, P = 0.064). In the box-and-whisker plots, the horizontal bar indicates the median, the box edges represent the 25th and 75th percentiles, and the whiskers represent the 10th and 90th percentiles. *$P \leq 0.05$, by paired, 2-tailed Student's t test.

Methods

Participants. This study included 24 patients with AN and 30 controls with normal weight as well as 25 controls with obesity. All participants were women. Patients with AN were recruited consecutively from our in- and outpatient departments after giving their written informed consent. Patients had to meet the diagnostic criteria for AN (Diagnostic and Statistical Manual of Mental Disorders IV [DSM-IV] criteria) and have a BMI between 13 kg/m^2 and17.5 kg/m^2. Normal-weight controls had a BMI between 18.5 kg/m^2 and 25 kg/m^2 and no lifetime or current medical illness that could potentially affect appetite or weight. Control participants with obesity had a BMI between 30 kg/m^2 and 45 kg/m^2 and no lifetime or current medical illness that could potentially affect appetite or weight (including an eating disorder diagnosis). Exclusion criteria were a history of head injury or operation, neurological disorder, psychosis, bipolar disorder, current or lifetime substance abuse, borderline personality disorder, or the current use of psychotropic medications, with the exception of selective serotonin reuptake inhibitors (SSRIs) (4 patients with AN were currently taking SSRI medications, but none of the participants from either control group was taking psychotropic medications). Normal-weight control participants were matched to patients with AN and control participants with obesity with regard to age and education level. However, there was a significant age difference between patients with AN and control participants with obesity (Table 1). In the AN group, 17 patients were diagnosed with restricting-type AN and 7 with binge/purging-type AN.

Procedures. We used a randomized, single-blind, crossover experimental fMRI design of intragastric glucose versus water infusion via a nasogastric tube. All sessions took place at the same time of the day (12:00 pm) with a 1-week gap between the 2 sessions. All participants were asked to fast overnight (no food or caloric beverages later than 8:00 pm). Immediately before and after the fMRI scanning, the participants provided hunger and mood ratings. A nasogastric tube for liquid administration was positioned at least 1 hour before the subject entered the scanner. A fine-bore nasogastric feeding tube (Flocare Nutrisoft, Nutricia GmbH) was positioned with its tip in the stomach 5 cm below the xiphoid process and fixed with adhesive tape to the subject's face. Accurate positioning was verified by aspirating gastric contents. Participants then received either 75 g glucose dissolved in 300 mL water or an equivalent amount of water (300 mL) without glucose. Injection of fluids took a maximum of 2 minutes.

Blood samples were obtained at 2 time points — 30 minutes before liquid infusion and 45 minutes after liquid infusion — to determine the participants' plasma glucose, insulin, and ghrelin concentrations (see below). This time frame was chosen to obtain estimates of hormonal satiety parameters in close temporal alignment with our fMRI sequence and because blood glucose values are expected to peak after a period of roughly 30 to 45 minutes following the infusion of 75 g glucose (43). Liquids were administered by the experimenter after a 5-minute baseline scan. To ensure concealment of the liquid type, the syringes used for the application were wrapped with tape. Following injection, participants were scanned for 30 minutes to assess brain-related activity during the digestion of glucose or water. Following this, an experimental food cue reactivity task lasting 15 minutes was performed, and the results of the latter are reported elsewhere (44, 45). The nasogastric tube was removed after the participant left the scanner; 10 mL water was injected into the feeding tube before removal to prevent oral detection of the liquid type. The feasibility of the procedure and blinding were successfully validated before the application.

Blood sampling. Two blood samples were collected 30 minutes before liquid infusion and 45 minutes after infusion for the measurement of peripheral glucose, insulin, and total and active acyl-ghrelin. Blood samples were collected using 21-gauge Multifly needles (Sarstedt AG) and kept on ice in chilled tubes containing EDTA-2Na and serine protease inhibitor (for ghrelin measurement, Pefabloc SC, Millipore Sigma). Blood samples were then centrifuged at 2000 × g for 15 minutes and stored at –80°C for later measurement. For the measurement of total and active ghrelin, the plasma tubes were acidified with HCl to

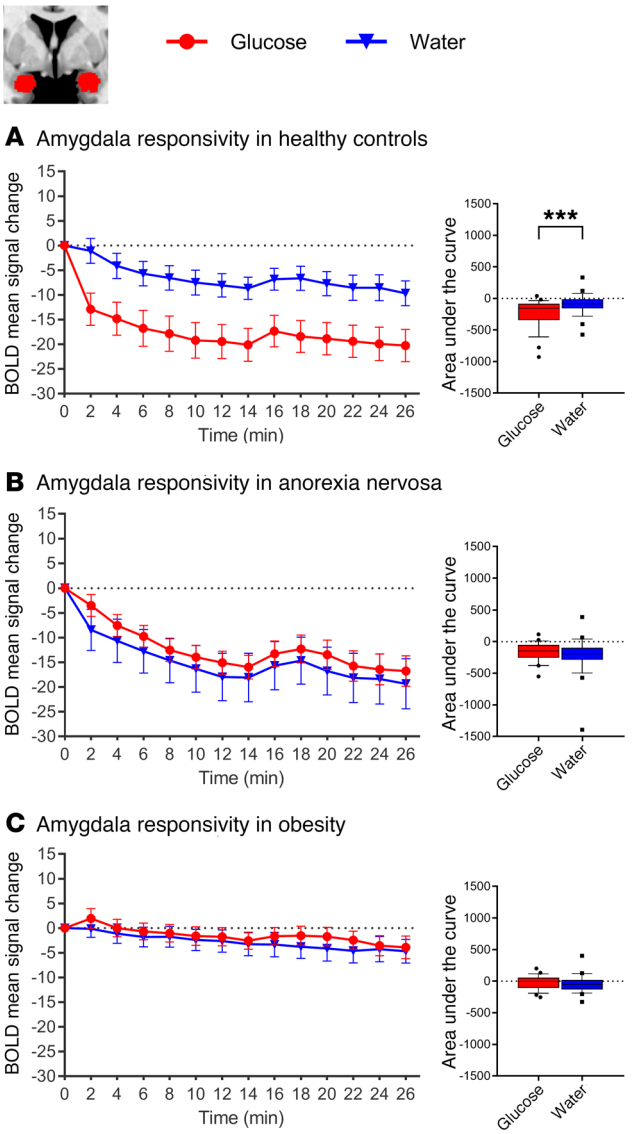

Figure 4. Changes in BOLD signal over time in response to glucose and water infusion in the amygdala. BOLD signal response in the amygdala ROI (automatic segmentation using FreeSurfer) during glucose and water infusion. Significant differences in AUC between conditions were observed in (**A**) normal-weight controls (t_{27} = 3.54, P = 0.001), but not in (**B**) patients with AN (t_{23} = 0.9, P = 0.378) or (**C**) controls with obesity (t_{23} = 0.37, P = 0.71). In the box-and-whisker plots, the horizontal bar indicates the median, the box edges represent the 25th and 75th percentiles, and the whiskers represent the 10th and 90th percentiles. ***$P \leq 0.001$, by paired, 2-tailed Student's t test.

a final concentration of 0.05 N to preserve the integrity of the ghrelin. The plasma glucose concentration was measured using the glucose oxidase method (Merck KGaA). Plasma insulin and total and active ghrelin were measured using commercially available kits from Merck Millipore (Merck KGaA). Homeostatic model assessment of insulin resistance (HOMA-IR) was obtained by multiplying the insulin concentration by the glucose concentration and dividing the result by 405.

fMRI acquisition. Functional imaging was performed on a 3-Tesla Tim Trio Scanner (Siemens Medical) using a 32-channel head coil. A high-resolution, gradient-recalled EPI acquisition following the sequence parameter sets previously used for other groups was used (46, 47). Thirty-five axial slices centered at the hypothalamus and aligned along the anterior commissure–posterior commissure (AC-PC) line were acquired with a slice thickness of 2 mm and no gap. The field of view was 10.4 cm × 10.4 cm with a matrix size of 52 × 52 and a flip angle of 80°. This high spatial resolution acquisition scheme significantly reduces signal drop-out in the amygdala-hypothalamus region (48). Parallel imaging with a GRAPPA (generalized autocalibrating partially parallel acquisition) factor of 2 was used to enable both a echo time (TE) of 30 ms and a repetition time (TR) of 2260 ms at this high spatial resolution. The field of view of the high-resolution echo-planar imaging (EPI) sequence used provided reduced brain coverage, with regions located dorsally from the corpus callosum left out (see Supplemental Figure 2 for a depiction of the mean EPI brain coverage and resulting second-level mask used for group comparisons in the connectivity analysis). Additionally, a T1-weighted high-resolution anatomical image with 192 slices (1 × 1 × 1 mm voxel size, TR = 1900 ms, TE = 2.52 ms, flip angle = 9°, field of view = 25.6 cm × 25.6 cm) was acquired for anatomical reference.

Region of interest–based MRI analysis. To assess hypothalamic activity, the hypothalamus of each individual was manually segmented, and preinfusion and postinfusion scans were divided into 14 consecutive 2-minute time bins. For each subject and each condition (glucose, water), the signal averages within the hypothalamus region of interest (ROI) during the 13 postinfusion time bins were compared with the baseline average. After motion correction of fMRI images by realignment to the mean image, the hypothalamus of each individual was manually segmented in a single-blinded fashion using the respective anatomical image in native space following predefined criteria (ref. 9 and Supplemental Figure 1). Additional reward-related brain regions (NAcc, amygdala) were automatically segmented from individual brain scans using FreeSurfer (http://surfer.nmr.mgh.harvard.edu). Furthermore, a reference region of about the same size as the hypothalamus ROI was drawn in the occipital cortex of each individual. The mean signal of this reference area was subtracted from that in the hypothalamus to correct for global signal drift. To assess differences between conditions and groups, we compared the AUC, which calculated using the trapezoidal rule by approximating the region under the graph. AUC values were compared using a repeated-measures ANOVA, and post hoc tests were performed using 2-sample t tests. To assess structural brain differences between groups, we calculated the hypothalamic volume (as a percentage of total brain volume) as well as the volume of the total gray and white matter for each participant, and compared the mean volume of each group using an independent-sample t test. The relation between hypothalamic activity and hormonal satiety parameters was assessed using the Pearson product-moment correlation coefficient (2-tailed, $P < 0.05$).

Seed-based connectivity analysis. A whole-brain connectivity analysis as implemented in the CONN toolbox, version 17 (https://www.nitrc.org/projects/conn; ref. 49) was performed to assess functional coupling between the hypothalamus and the rest of the brain (i.e., voxels contained within the reduced brain mask; see Supplemental Figure 2) in response to the glucose and water infusion. FMRI data were preprocessed using SPM8-based routines (http://www.fil.ion.ucl.ac.uk/spm/software/spm8). To account for magnetic field equilibration, 4 volumes from the start of each functional run were excluded from the analysis. All functional images were inspected manually for artifacts. Functional scans were slice-time corrected with reference to the first

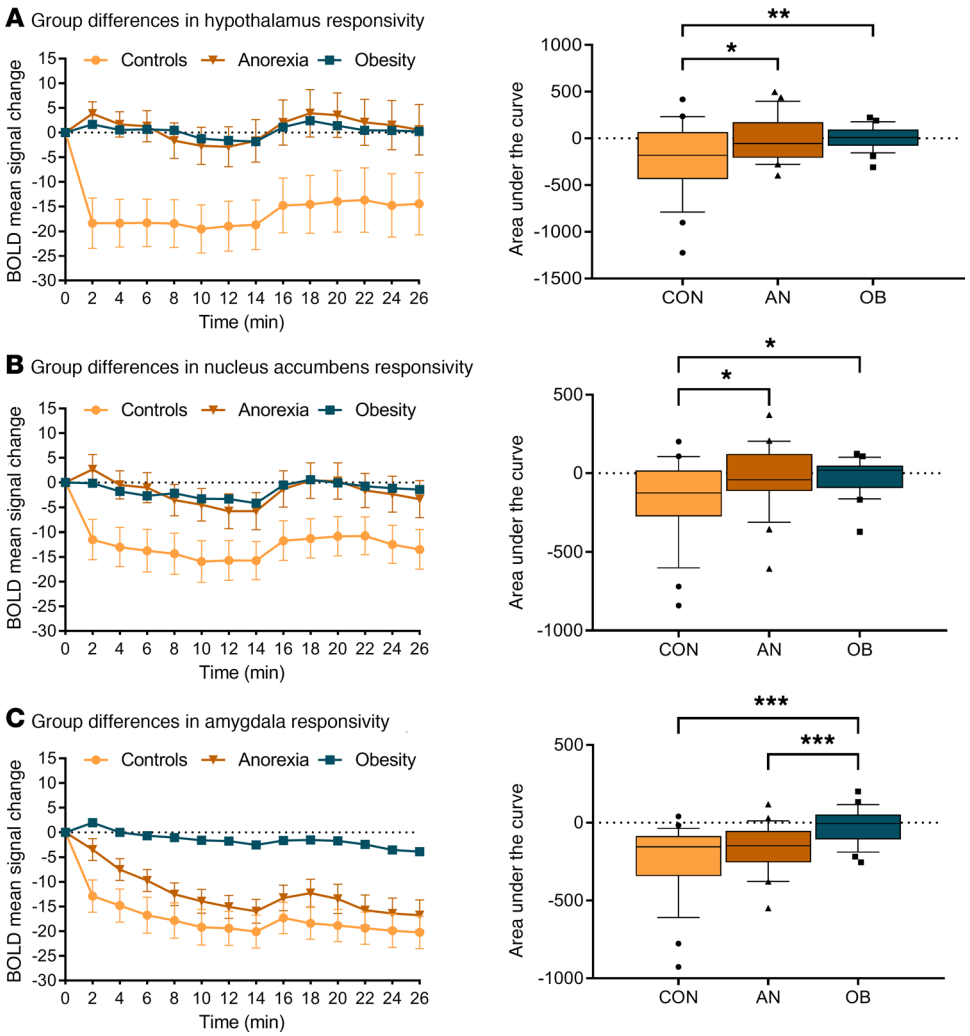

Figure 5. Differences between groups in BOLD signal response during glucose infusion. (**A**) Group differences in hypothalamus reactivity during glucose infusion (comparison between all 3 groups: $F_{2,73}$ = 5.74, P = 0.005, by repeated-measures ANOVA). (**B**) Differences between groups in BOLD signal response in the NAcc during glucose infusion (comparison between all 3 groups: $F_{2,73}$ = 4.32, P = 0.017, by repeated-measures ANOVA; normal-weight controls vs. patients with AN: t_{50} = 2.12, P = 0.038; normal-weight controls vs. controls with obesity: t_{50} = 2.57, P = 0.013; and controls with obesity vs. patients with AN: t_{46} = −0.15, P = 0.882, by Student's t test). (**C**) Differences between groups in BOLD signal response in the amygdala during glucose infusion (comparison between all 3 groups: $F_{2,73}$ = 10.84, P < 0.001). No significant differences were observed between normal-weight controls and patients with AN (t_{50} = 1.66, P = 0.103), but significant differences were observed between normal-weight controls and controls with obesity (t_{50} = −4.35, P < 0.001) and between controls with obesity and patients with AN (t_{46} = −3.59, P < 0.001). In the box-and-whisker plots, the horizontal bar indicate the median, the box edges represent the 25th and 75th percentiles, and the whiskers represent the 10th and 90th percentiles. *P ≤ 0.05, **P ≤ 0.01, and ***P ≤ 0.001, by post hoc 2-sample, 2-tailed Student's t test.

slice using SPM8's Fourier phase-shift interpolation. Images were then realigned, with the allowed motion limited to ±4 mm translation and ±3° of rotation over the entire experiment. One normal-weight control had to be excluded because of excessive head movement during scanning; 1 normal-weight control and 1 control with obesity had to be excluded because of technical difficulties during scanning. Furthermore, the Artifact Detection Tools (ART) toolbox (http://www.nitrc.org/projects/artifact_detect) was used for outlier detection, and single scans identified as invalid outliers were removed from subsequent analysis. Individual T1 images were coregistered with the mean T2* images and subsequently segmented into gray matter (GM), white matter (WM), and cerebrospinal fluid (CSF) partitions and were spatially normalized to the Montreal Neurological Institute (MNI) standardized space (http://www.mni.mcgill.ca). The functional volumes were resampled to a 1 × 1 × 1 mm^3 voxel size and spatially smoothed with an 8-mm full-width half-maximum (FWHM) isotropic Gaussian kernel.

In the subsequent seed-to-voxel analysis, the temporal correlation between the BOLD signal from the hypothalamus seed to all other voxels in the brain was computed. Head motion measured in 6 dimensions was included as a nuisance variable; furthermore, a component-based noise reduction method (CompCor; ref. 50) removed principal components on the basis of both WM and CSF signals and accounted for physiological noise, such as heart rate and respiration. We then used the individually segmented masks of the hypothalamus as seed masks at the individual level. Time series of each condition were extracted from each voxel within the ROI in native space. Specifically, we used the realigned fMRI data stemming from the time-series analysis to extract ROI data. This allowed us to extract BOLD data in the original native space of each participant,

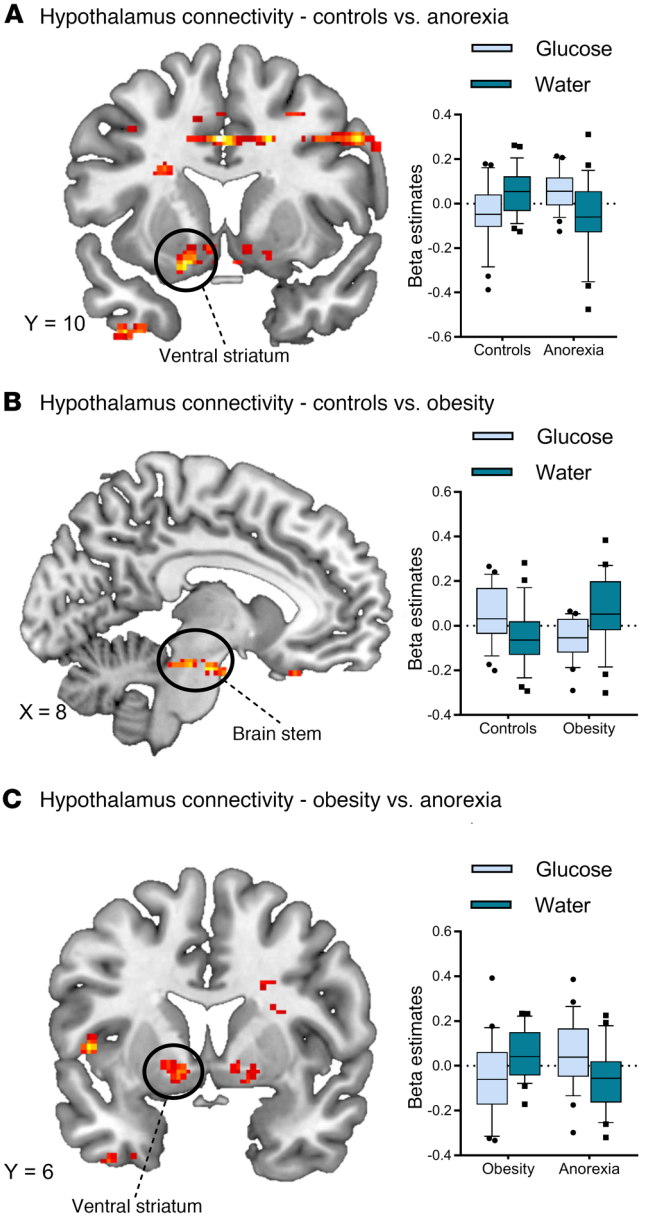

Figure 6. Satiety state–dependent functional connectivity of the hypothalamus. (**A**) Differences between normal-weight controls and patients with AN in functional connectivity between the hypothalamus and the left ventral striatum (glucose, t_{50} = –3.22, P = 0.002; water, t_{50} = 2.67, P = 0.01). (**B**) Differences between normal-weight controls and controls with obesity in functional connectivity between the hypothalamus and brainstem (glucose: t_{50} = 3.44, P = 0.001; water: t_{50}= –2.51, P = 0.015). (**C**) Differences between patients with AN and controls with obesity in functional connectivity between the hypothalamus and left ventral striatum (glucose, t_{46} = 2.33, P = 0.024; water, t_{46}= –2.96, P = 0.005). All whole-brain results are reported at a threshold of P < 0.05 corrected for multiple comparisons using FWE correction for small volumes and a cluster-defining threshold of k > 30 voxel minimal cluster size. In the box-and-whisker plots, the horizontal bar indicates the median, the box edges represent the 25th and 75th percentiles, and the whiskers represent the 10th and 90th percentiles.

thereby increasing special fidelity. Block regressors corresponding to the 14 consecutive 2-minute time bins were convolved with a canonical hemodynamic response function and subsequently temporally bandpass filtered (0.008 < f < 0.09) to remove low-frequency drift and high-frequency noise. For each participant, bivariate Pearson correlation analyses were performed to estimate the connection from the seed hypothalamus ROI to other voxels in the brain using the preprocessed (i.e., normalized and smoothed data) fMRI data. The resulting statistical maps were analyzed in a random-effects group analysis to compare connectivity profiles between groups. Specifically, we performed a repeated-measures ANOVA with liquid type and time point as within-subject factors and group as a between-subjects factor. Age as well as depression scores (as assessed by the Beck Depression Inventory II; ref. 51) were included as covariates of no interest for between-groups analyses. Whole-brain second-level results are reported for the main effect of liquid type (i.e., satiety). Statistical inference was based on a significance threshold of P < 0.05 corrected for multiple comparisons using FWE correction for small volumes and a cluster-defining threshold of k >30 voxel minimal cluster size. Post hoc analyses were performed to determine the direction of significant ANOVA results; β values (parameter estimates) were extracted in SPM (https://www.fil.ion.ucl.ac.uk/spm/) and subsequently analyzed using paired Student's t tests (2-tailed) for within-group results and 2-sample Student's t tests (2-tailed) for between-groups results. The significance threshold was set at P < 0.05.

Statistics. Within-group analyses of hypothalamic reactivity to glucose and water were compared using 2-tailed, paired Student's t tests (P < 0.05). Between-groups analyses of hypothalamic reactivity were performed using a repeated-measures ANOVA with group as a between-subjects factor and post hoc 2-sample, 2-tailed Student's t tests (P < 0.05). A random-effects group analysis using a repeated-measures ANOVA with group as a between-subjects factor was used for the seed-based connectivity analysis; age and depression scores were included as covariates of no interest for between-groups analyses. Results were deemed significant at P < 0.05, corrected for multiple comparisons using FWE correction for small volumes and a cluster-defining threshold of k >30 voxel minimal cluster size. β Values were analyzed using paired, 2-tailed Student's t tests for within-group results and 2-sample, 2-tailed Student's t tests for between-groups results. The significance threshold was set at P < 0.05. Behavioral data were analyzed using Pearson's χ^2 test for independence (guess of liquid type, P < 0.05) and a repeated-measures ANOVA with group as a between factor and post hoc 2-sample, 2-tailed Student's t tests (hunger ratings, P < 0.05). Hormonal satiety parameters were analyzed using a repeated-measures ANOVA and post hoc paired as well as 2-sample, 2-tailed Student's t tests (P < 0.05). Correlations were performed using the Pearson product-moment correlation coefficient (2-tailed, P < 0.05).

Study approval. The medical ethics committee of the Medical Faculty Heidelberg at the Ruprecht-Karls-University in Heidelberg, Germany, approved this study (protocol number S-373/2014), and written informed consent was obtained from all participants.

Author contributions

JJS, MB, HP, LPK, WH, and HCF designed the research. MSS, EM, SS, and NL collected the data. JJS, MAS, and HCF analyzed the data. JJS, MB, HP, LPK, WH, and HCF wrote the manuscript.

Address correspondence to: Hans-Christoph Friederich, Centre for Psychosocial Medicine, General Internal Medicine and Psychosomatics, University Hospital Heidelberg, Im Neuenheimer Feld 410, 69120 Heidelberg, Germany. Phone: 49.6221.56.8649; Email: hans-christoph.friederich@med.uni-heidelberg.de.

1. Zipfel S, Giel KE, Bulik CM, Hay P, Schmidt U. Anorexia nervosa: aetiology, assessment, and treatment. *Lancet Psychiatry*. 2015;2(12):1099–1111.
2. Mayer EA. Gut feelings: the emerging biology of gut-brain communication. *Nat Rev Neurosci*. 2011;12(8):453–466.
3. Kaye WH, Fudge JL, Paulus M. New insights into symptoms and neurocircuit function of anorexia nervosa. *Nat Rev Neurosci*. 2009;10(8):573–584.
4. Estour B, et al. Differentiating constitutional thinness from anorexia nervosa in DSM 5 era. *Psychoneuroendocrinology*. 2017;84:94–100.
5. Monteleone P, Maj M. Dysfunctions of leptin, ghrelin, BDNF and endocannabinoids in eating disorders: beyond the homeostatic control of food intake. *Psychoneuroendocrinology*. 2013;38(3):312–330.
6. Frank GKW, DeGuzman MC, Shott ME. Motivation to eat and not to eat – the psycho-biological conflict in anorexia nervosa. *Physiol Behav*. 2019;206:185–190.
7. Berthoud HR, Münzberg H, Morrison CD. Blaming the brain for obesity: integration of hedonic and homeostatic mechanisms. *Gastroenterology*. 2017;152(7):1728–1738.
8. Burger KS, Berner LA. A functional neuroimaging review of obesity, appetitive hormones and ingestive behavior. *Physiol Behav*. 2014;136:121–127.
9. Matsuda M, et al. Altered hypothalamic function in response to glucose ingestion in obese humans. *Diabetes*. 1999;48(9):1801–1806.
10. Jastreboff AM, et al. Altered brain response to drinking glucose and fructose in obese adolescents. *Diabetes*. 2016;65(7):1929–1939.
11. Berthoud HR. Metabolic and hedonic drives in the neural control of appetite: who is the boss? *Curr Opin Neurobiol*. 2011;21(6):888–896.
12. Ladenheim EE. Gastrointestinal regulatory peptides and central nervous system mechanisms of weight control. *Curr Opin Endocrinol Diabetes Obes*. 2012;19(1):13–18.
13. Baldo BA, Kelley AE. Discrete neurochemical coding of distinguishable motivational processes: insights from nucleus accumbens control of feeding. *Psychopharmacology (Berl)*. 2007;191(3):439–459.
14. de Araujo IE, Lin T, Veldhuizen MG, Small DM. Metabolic regulation of brain response to food cues. *Curr Biol*. 2013;23(10):878–883.
15. Berridge KC. Food reward: brain substrates of wanting and liking. *Neurosci Biobehav Rev*. 1996;20(1):1–25.
16. Zanchi D, et al. The impact of gut hormones on the neural circuit of appetite and satiety: A systematic review. *Neurosci Biobehav Rev*. 2017;80:457–475.
17. Burdakov D, Luckman SM, Verkhratsky A. Glucose-sensing neurons of the hypothalamus. *Philos Trans R Soc Lond, B, Biol Sci*. 2005;360(1464):2227–2235.
18. Page KA, et al. Effects of fructose vs glucose on regional cerebral blood flow in brain regions involved with appetite and reward pathways. *JAMA*. 2013;309(1):63–70.
19. Smeets PA, de Graaf C, Stafleu A, van Osch MJ, van der Grond J. Functional MRI of human hypothalamic responses following glucose ingestion. *Neuroimage*. 2005;24(2):363–368.
20. van Opstal AM, Westerink AM, Teeuwisse WM, van der Geest MA, van Furth EF, van der Grond J. Hypothalamic BOLD response to glucose intake and hypothalamic volume are similar in anorexia nervosa and healthy control subjects. *Front Neurosci*. 2015;9:159.
21. Konturek SJ, Konturek JW, Pawlik T, Brzozowski T. Brain-gut axis and its role in the control of food intake. *J Physiol Pharmacol*. 2004;55(1 Pt 2):137–154.
22. Field BC, Chaudhri OB, Bloom SR. Bowels control brain: gut hormones and obesity. *Nat Rev Endocrinol*. 2010;6(8):444–453.
23. Morton GJ, Cummings DE, Baskin DG, Barsh GS, Schwartz MW. Central nervous system control of food intake and body weight. *Nature*. 2006;443(7109):289–295.
24. Timper K, Brüning JC. Hypothalamic circuits regulating appetite and energy homeostasis: pathways to obesity. *Dis Model Mech*. 2017;10(6):679–689.
25. Thaler JP, et al. Obesity is associated with hypothalamic injury in rodents and humans. *J Clin Invest*. 2012;122(1):153–162.
26. Frank GK, Shott ME, Riederer J, Pryor TL. Altered structural and effective connectivity in anorexia and bulimia nervosa in circuits that regulate energy and reward homeostasis. *Transl Psychiatry*. 2016;6(11):e932.
27. Florent V, et al. Hypothalamic structural and functional imbalances in anorexia nervosa [published online September 5, 2019]. *Neuroendocrinology*. https://doi.org/10.1159/000503147.
28. Miljic D, et al. Ghrelin has partial or no effect on appetite, growth hormone, prolactin, and cortisol release in patients with anorexia nervosa. *J Clin Endocrinol Metab*. 2006;91(4):1491–1495.
29. Friederich HC, Wu M, Simon JJ, Herzog W. Neurocircuit function in eating disorders. *Int J Eat Disord*. 2013;46(5):425–432.
30. Siep N, Roefs A, Roebroeck A, Havermans R, Bonte ML, Jansen A. Hunger is the best spice: an fMRI study of the effects of attention, hunger and calorie content on food reward processing in the amygdala and orbitofrontal cortex. *Behav Brain Res*. 2009;198(1):149–158.
31. Kaye WH, Wierenga CE, Bailer UF, Simmons AN, Bischoff-Grethe A. Nothing tastes as good as skinny feels: the neurobiology of anorexia nervosa. *Trends Neurosci*. 2013;36(2):110–120.
32. Goldzak-Kunik G, Friedman R, Spitz M, Sandler L, Leshem M. Intact sensory function in anorexia nervosa. *Am J Clin Nutr*. 2012;95(2):272–282.
33. Berthoud HR, Morrison C. The brain, appetite, and obesity. *Annu Rev Psychol*. 2008;59:55–92.
34. Stoeckel LE, Weller RE, Cook EW, Twieg DB, Knowlton RC, Cox JE. Widespread reward-system activation in obese women in response to pictures of high-calorie foods. *Neuroimage*. 2008;41(2):636–647.
35. Smith DG, Robbins TW. The neurobiological underpinnings of obesity and binge eating: a rationale for adopting the food addiction model. *Biol Psychiatry*. 2013;73(9):804–810.
36. Simon JJ, et al. Impaired cross-talk between mesolimbic food reward processing and metabolic signaling predicts body mass index. *Front Behav Neurosci*. 2014;8:359.
37. Arnoni-Bauer Y, et al. Is it me or my hormones? Neuroendocrine activation profiles to visual food stimuli across the menstrual cycle. *J Clin Endocrinol Metab*. 2017;102(9):3406–3414.
38. Bichet DG. Vasopressin and the regulation of thirst. *Ann Nutr Metab*. 2018;72 Suppl 2:3–7.
39. Watts AG, Sanchez-Watts G, Kelly AB. Distinct patterns of neuropeptide gene expression in the lateral hypothalamic area and arcuate nucleus are associated with dehydration-induced anorexia. *J Neurosci*. 1999;19(14):6111–6121.
40. Ferrario CR, et al. Homeostasis meets motivation in the battle to control food intake. *J Neurosci*. 2016;36(45):11469–11481.
41. Bentsen MA, Mirzadeh Z, Schwartz MW. Revisiting how the brain senses glucose – and why. *Cell Metab*. 2019;29(1):11–17.
42. Watson HJ, et al. Genome-wide association study identifies eight risk loci and implicates metabo-psychiatric origins for anorexia nervosa. *Nat Genet*. 2019;51(8):1207–1214.
43. Zhou W, Gu Y, Li H, Luo M. Assessing 1-h plasma glucose and shape of the glucose curve during oral glucose tolerance test. *Eur J Endocrinol*. 2006;155(1):191–197.
44. Stopyra MA, et al. The effect of intestinal glucose load on neural regulation of food craving [published online Apr 15, 2019]. *Nutr Neurosci*. https://doi.org/10.1080/1028415X.2019.1600275.
45. Stopyra MA, et al. The influence of homeostatic mechanisms on neural regulation of food craving in anorexia nervosa [published online Jan 14, 2019]. *Psychol Med*. https://doi.org/10.1017/S0033291719003970.
46. Robinson S, Windischberger C, Rauscher A, Moser E. Optimized 3 T EPI of the amygdalae. *Neuroimage*. 2004;22(1):203–210.
47. Karlsson KA, Windischberger C, Gerstl F, Mayr W, Siegel JM, Moser E. Modulation of hypothalamus and amygdalar activation levels with stimulus valence. *Neuroimage*. 2010;51(1):324–328.
48. Robinson SD, Pripfl J, Bauer H, Moser E. The impact of EPI voxel size on SNR and BOLD sensitivity in the anterior medio-temporal lobe: a comparative group study of deactivation of the Default Mode. *MAGMA*. 2008;21(4):279–290.
49. Whitfield-Gabrieli S, Nieto-Castanon A. CONN: a functional connectivity toolbox for correlated and anticorrelated brain networks. *Brain Connect*. 2012;2(3):125–141.
50. Behzadi Y, Restom K, Liau J, Liu TT. A component based noise correction method (CompCor) for BOLD and perfusion based fMRI. *Neuroimage*. 2007;37(1):90–101.
51. Hautzinger M, Keller F, Kühner C, Beck AT. *Beck Depressions-Inventar: BDI II. Revision*. Harcourt Test Services; 2006.